Bursty Impulse Noise Detection by Compressed Sensing

Lutz Lampe
University of British Columbia, Vancouver, BC, Canada, lampe@ece.ubc.ca

***Abstract*—Impulse noise (IN) is one of the major impairments for data transmission over power lines. For power line communications (PLC) systems with bandwidths in the high kHz to MHz range, IN occurs in bursts. As long as those bursts are sufficiently short compared to a signal-processing (e.g. coding) frame, there is hope to successfully mitigate IN. In this paper, we introduce a new IN mitigation technique that is based on the application of block-based compressed sensing (CS). It makes use of null-subcarriers in PLC orthogonal frequency division multiplexing (OFDM) transmission systems and the burst structure of IN to detect the location and the values of IN samples in the received signal. We also devise a semi-analytical error-rate performance evaluation for coded OFDM over IN channels, which allows insights into how CS-based IN detection can be used for improved reliability of transmission. Numerical results for typical PLC transmission settings demonstrate the efficacy of the proposed application of CS for IN detection.**

***Index Terms*—Power line communications (PLC), impulse noise, compressed sensing, orthogonal frequency division multiplexing (OFDM), error-rate analysis, coding.**

I. Introduction

Data communication over power lines is attractive for its cost-efficient installation (no need to lay wires, no need to purchase spectrum), high penetration of the power distribution grid, and ease of use for customers (one wire to connect them all). However, there are a number of serious challenges for power line communications (PLC) resulting from the use of networks designed to carry the AC or DC mains signal

One of these challenges concerns the noise scenario of PLC transmission, which is considerably richer than captured by the conventional additive white Gaussian noise (AWGN) model [1], [2], [3, Chapter 2.6]. In particular, the presence of impulse and narrowband noise render reliable communication difficult. While the narrowband noise is dealt with through switching or receiver-side notching of frequency bands, impulse noise (IN) is often mitigated by relatively simple clipping or clipping and nulling [4], or more sophisticated parametric [5] and iterative [6], [7] IN suppression schemes. More recently, Caire et al. [8] proposed the application of compressed sensing (CS) [9]–[11] to cancel IN for orthogonal frequency division multiplexing (OFDM) transmission. More specifically, it was suggested to exploit null subcarriers to setup an underdetermined system of linear equations, from which IN is estimated making use of the fact that IN realizations are "sparse" (otherwise it would not be "impulse" noise).

In this paper, we adopt the CS-based approach from [8] and extend it to the case of bursty IN. That is, IN is assumed to occur in bursts and corrupt blocks of received OFDM signal samples. This assumption is very well justified considering Gaussian-Markov IN models for broadband PLC [2]. Of course, if the length of IN bursts is of the same order as the length of an entire OFDM symbol, IN cancellation methods operating on individual OFDM symbols cannot be successful. (In this case, coding at the application layer, spanning multiple OFDM symbols is an interesting alternative [12].) So our approach provides benefits if the signal bandwidth and IN realizations are such that the sampled IN signal is in-between the extreme cases of i.i.d. IN [8] and long IN bursts that destroy entire OFDM symbols [12]. Our approach to take the bursty nature of IN into account relies on the application of CS for block-sparse signals [13], [14]. Furthermore, to provide quantitative error-rate results that indicate what burst lengths could be dealt with by a coded OFDM system and as well as the attainable performance gains by CS-based IN detection, we also provide semi-analytical error-rate expressions. These expressions are derived from a union-bound approach and thus are tight for moderately complex coding schemes, such as convolutional coding. We present numerical results for PLC OFDM transmission according to IEEE 1901 standard [15] and sample channels from [16] that demonstrate that the proposed CS-based processing is effective for IN detection and that subsequent IN cancellation or suppression significantly improves transmission reliability.

The remainder of this paper is organized as follows. In Section II, we introduce the system model of OFDM transmission over power line channels with additive IN. The CS-based processing of IN is presented in Section III, and the error-rate analysis is derived in Section IV. In Section V, we show numerical results to highlight the effectiveness of the proposed CS application. Finally, conclusions are given in Section VI.

II. System Description

We consider a conventional OFDM transmission system based on inverse discrete Fourier transform (IDFT) and DFT operations at the transmitter and receiver, respectively. The relevant portions of the transmitter and receiver block diagram are shown in Figure 1.

A. Transmitter

At the transmitter, a binary data stream $\boldsymbol{b} = [b_1, \ldots, b_{L_b}]^T$ of length $L_b = R_c R_m N$ is encoded into a codeword $\boldsymbol{c} = [c_1, \ldots, c_{L_c}]^T$ of length $L_c = R_m N$, where R_c and R_m denote code and modulation rate, respectively. While any code including turbo-convolutional and low-density parity check (LDPC) codes selected (optionally) in, e.g., IEEE 1901 and ITU-T G.9960 standards could be considered, as the proposed CS-based IN detection method is independent of the applied coding scheme, in this work we assume the

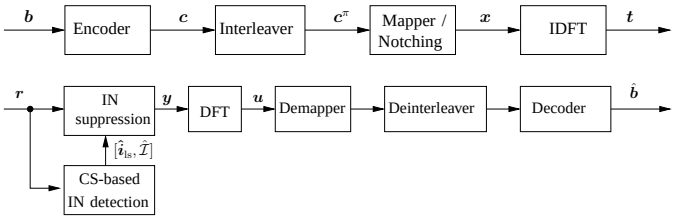

Fig. 1. Block-diagram of the OFDM transmitter (top) and receiver (bottom).

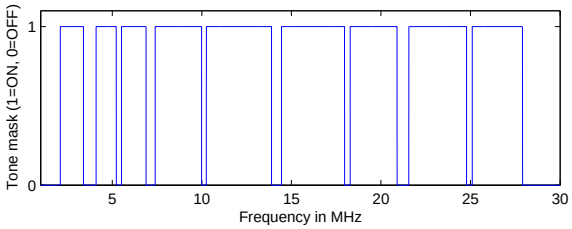

Fig. 2. Default broadcast tone mask (ON/OFF of OFDM subcarriers) for the OFDM physical layer of IEEE 1901 for North America [15, Table 13-39].

application of convolutional coding. Convolutional coding is also very popular for practical PLC transmission systems, including iAd's DLC2000, G3-PLC, and PRIME for low-frequency narrowband PLC, and the wavelet physical layer of IEEE 1901 (typically supported by an outer Reed-Solomon code).

The encoder output is interleaved into the vector $\boldsymbol{c}^{\pi}$, whose elements are then mapped to N signal points $\boldsymbol{x} = [x_1, \ldots, x_N]^T$. The signal points are taken from the 2^{R_m}-ary quadrature-amplitude modulation (QAM) constellation $\mathcal{X}$. For simplicity, we assume that the same constellation is used for all OFDM subcarriers, but we note that the proposed CS-based IN detection method operates irrespective of whether bit loading is applied. The vector $\boldsymbol{x}$ of data symbols is expanded to the K-dimensional vector $\boldsymbol{x'} = [x'_1, \ldots, x'_K]^T$ by introducing $K-N$ zeros, where x'_i is transmitted over the ith OFDM subcarrier (a.k.a. OFDM tone). Such null-subcarriers are used to avoid interference with radio services, and are also a possible means to enable coexistence among PLC systems. As an example, Figure 2 shows the default broadcast tone mask (ON/OFF of OFDM subcarriers) for the OFDM physical layer of IEEE 1901 for North America [15, Table 13-39].

The modulated OFDM symbols are converted into the time-domain vector

$$\boldsymbol{t} = \boldsymbol{F}^H \boldsymbol{x'} \ , \tag{1}$$

where $\boldsymbol{F}$ is the $K \times K$ DFT matrix. Finally (not included in Figure 1), a cyclic prefix (CP) is added and pulse shaping (digital-to-analog conversion (DAC)) is applied.

Let us denote the set of data- and null-subcarriers as $\mathcal{T}$ and $\mathcal{T}^{\mathrm{c}}$, respectively. For later use, we partition the DFT matrix $\boldsymbol{F}$ into the $(K-N) \times K$ partial DFT matrix $\boldsymbol{F}_1$ consisting of the $K-N$ rows from $\boldsymbol{F}$ that are at positions $i \in \mathcal{T}^{\mathrm{c}}$, and the $N \times K$ partial DFT matrix $\boldsymbol{F}_2$ consisting of the remaining N rows from $\boldsymbol{F}$ at positions $i \in \mathcal{T}$.

B. Channel

For our purposes, it is sufficient to consider the discrete-time complex baseband equivalent channel that results when including the effects of CP-addition and DAC at the transmitter and analog-to-digital conversion (ADC) and CP-removal at the receiver into the channel model. Assuming that the CP is sufficiently long (essentially as long as the channel impulse response), the vector of K received time-domain samples can be written as

$$\boldsymbol{r} = \boldsymbol{H}_{\mathrm{cyc}} \boldsymbol{t} + \boldsymbol{n} + \boldsymbol{i} \ , \tag{2}$$

where $\boldsymbol{H}_{\mathrm{cyc}}$ is a $K \times K$ column-circulant matrix with the first column equal to the discrete-time channel impulse response [17, Section 4.1] and $\boldsymbol{n}$ is a vector of independent complex AWGN samples with variance $\mathcal{N}_0$. In addition to the AWGN, we also include the effect of additive IN, whose samples are collected in the vector $\boldsymbol{i}$. With regards to the characteristics of $\boldsymbol{i}$ we make the assumptions that

(i) $\boldsymbol{i}$ is m-sparse, i.e., only a number $m \ll K$ of its elements are non-zero, and
(ii) the non-zero elements are grouped together.

These assumptions are valid considering that IN occurs in the form of short bursts or pulses in PLC systems [2]. The size of the bursts in number of samples depends on the OFDM-signal bandwidth, which varies over about three orders of magnitude ($\sim$50 kHz for low-frequency narrowband PLC to $\sim$50 MHz for broadband PLC), and of course on the specific IN realization. Assumptions (i) and (ii) make the noise signal $\boldsymbol{i}$ block-sparse [13], [14].

C. Receiver

As mentioned in the previous section, the receiver employs an ADC, discards the CP portion of the sampled signal, and processes the output $\boldsymbol{r}$ in (2). The vector $\boldsymbol{r}$ is used for detection of interference $\boldsymbol{i}$ by the CS-based IN-noise detection algorithm described in Section III (see Figure 1). We investigate two possible ways of processing the IN contaminated signal $\boldsymbol{r}$.

1) *IN suppression (i.e., erasure decoding):* The CS-based detection unit delivers an estimate $\hat{\mathcal{I}}$ of the support $\mathcal{I}$ of $\boldsymbol{i}$, i.e., the positions of non-zero elements of $\boldsymbol{i}$. The elements of $\boldsymbol{r}$ which are deemed corrupted by IN are then erased. That is, defining the $K \times K$ "erasure" matrix $\boldsymbol{E}$ as an identity matrix but with elements $e_{jj} = 0$ for $j \in \hat{\mathcal{I}}$, the interference-processed signal is given by

$$\boldsymbol{y} = \boldsymbol{E}\boldsymbol{r} \ . \tag{3}$$

2) *IN cancellation:* The CS-based detection unit delivers an estimate $\hat{\boldsymbol{i}}_{\mathrm{ls}}$ of $\boldsymbol{i}$, which is subtracted from $\boldsymbol{r}$. That is,

$$\boldsymbol{y} = \boldsymbol{r} - \hat{\boldsymbol{i}}_{\mathrm{ls}} \ . \tag{4}$$

The signal $\boldsymbol{y} = [y_1, \ldots, y_K]^T$ is input to the DFT, followed by the demapper, deinterleaver, and the decoder, which then produces an estimate $\hat{\boldsymbol{b}}$ for the transmitted message $\boldsymbol{b}$.

III. Compressed-Sensing-Based Impulse Noise Detection

In this section, we consider the estimation of $\boldsymbol{i}$ for IN cancellation (4) and its support $\mathcal{I}$ for interference suppression (3). To this end, we exploit the null-tones of the OFDM signal and apply concepts from compressed sensing (CS) [9]–[11]. The basic idea is similar to [8], but different from their scheme, we make specific use of the burst structure of IN.

A. Preprocessing

Considering the approximately Gaussian distribution of the time-domain transmit signal $\boldsymbol{t}$ (1) [18] and thus the component $\boldsymbol{H}_{\rm cyc}\boldsymbol{t}$ of $\boldsymbol{r}$ in (2), direct detection of $\boldsymbol{i}$ based on $\boldsymbol{r}$ using outlier detection methods (e.g. clipping or clipping and nulling [4] or more sophisticated variants) is prone to false alarm. To rid ourselves of the data signal, we focus on the unused OFDM subcarriers. That is, we generate

$$\begin{aligned}\boldsymbol{w} &= \boldsymbol{F}_1\boldsymbol{r} \\ &= \boldsymbol{F}_1\boldsymbol{i} + \tilde{\boldsymbol{n}}\ ,\end{aligned} \tag{5}$$

where $\tilde{\boldsymbol{n}} = \boldsymbol{F}_1\boldsymbol{n}$ is AWGN and the second line follows from $x_j = 0$ for $j \in \mathcal{T}^{\rm c}$.

B. CS Essentials

Let us consider the problem of detecting a μ-sparse κ-dimensional vector $\boldsymbol{a}$ from $\nu < \kappa$ noisy observations

$$\boldsymbol{b} = \boldsymbol{\Phi}\boldsymbol{a} + \boldsymbol{n}\ , \tag{6}$$

where $\boldsymbol{\Phi}$ is the $\nu \times \kappa$ measurement matrix and $\boldsymbol{n}$ is AWGN. Estimating $\boldsymbol{a}$ from noisy measurements $\boldsymbol{b}$ is an ill-posed problem since $\boldsymbol{\Phi}$ has a non-trivial null space, and $\boldsymbol{a} + \boldsymbol{v}$ for any vector $\boldsymbol{v}$ in this null space gives the same observation $\boldsymbol{b}$. However, the knowledge that the solution $\hat{\boldsymbol{a}}$ needs to be sparse enables us to resolve ambiguity. In fact, the basic tenet of CS is that under certain conditions on the measurement matrix $\boldsymbol{\Phi}$, $\boldsymbol{a}$ can be robustly recovered using polynomial time convex programming or greedy algorithms, if $\nu \propto \mu\log(\kappa/\mu)$ [9]–[11]. One popular convex programming algorithm is

$$\begin{aligned}&\min \|\boldsymbol{a}\|_1 \\ \text{s.t.}\quad &\|\boldsymbol{b} - \boldsymbol{\Phi}\boldsymbol{a}\|_2 \le \epsilon\ ,\end{aligned} \tag{7}$$

where ϵ is related to the variance of $\boldsymbol{n}$ [19]–[21].

The CS concept has recently been extended to block-sparse signals [13], [14]. That is, writing

$$\boldsymbol{a} = [\underbrace{a_1,\ldots,a_\delta}_{\boldsymbol{a}^T[1]},\ldots,\underbrace{a_{\kappa-\delta+1},\ldots,a_\kappa}_{\boldsymbol{a}^T[p]}]^T, \tag{8}$$

then only $q \ll p$ vectors $\boldsymbol{a}[j]$ have nonzero Euclidean norm. Then, instead of minimizing the ℓ_1-norm of $\boldsymbol{a}$ as in (7), the mixed ℓ_2/ℓ_1 norm

$$\sum_{j=1}^{p} \|\boldsymbol{a}[j]\|_2 \tag{9}$$

is minimized.

C. CS-based Detection

We observe that (5) is of the same type as (6) with the parameter relations $(\boldsymbol{b},\boldsymbol{a},\boldsymbol{n},\boldsymbol{\Phi},\kappa,\nu,\mu) \to (\boldsymbol{w},\boldsymbol{i},\tilde{\boldsymbol{n}},\boldsymbol{F}_1,K,K-N,m)$. Furthermore, $\boldsymbol{i}$ has a block-sparse structure similar to $\boldsymbol{a}$ in (8). That is, the nonzero elements of $\boldsymbol{i}$ occur in bursts, but the beginning and the length of bursts are unknown. Finally, while likely recovery for problems of the type (6) is proved for random measurement matrices, it turns out that good recovery results are obtained also for deterministic matrices such as $\boldsymbol{F}_1$ in (5), e.g., [22].

Following the relation between IN detection and block-sparse signal recovery shown above, we represent the IN signal as the block-vector

$$\boldsymbol{i} = [\underbrace{i_1,\ldots,i_\delta}_{\boldsymbol{i}^T[1]},\ldots,\underbrace{i_{K-\delta+1},\ldots,i_K}_{\boldsymbol{i}^T[p]}]^T. \tag{10}$$

The choice of the detection block-size δ will be discussed in Section V. Using this representation, and adopting [21, Section 4] (also [8]), we apply the following detection algorithm.

1) Solve

$$\begin{aligned}\hat{\boldsymbol{i}} = \min &\sum_{j=1}^{p} \|\boldsymbol{i}[j]\|_2 \\ \text{s.t.}\quad &\|\boldsymbol{w} - \boldsymbol{F}_1\boldsymbol{i}\|_2 \le \epsilon\end{aligned} \tag{11}$$

where ϵ is adjusted such that $\|\tilde{\boldsymbol{n}}\|_2 \le \epsilon$ with probability 0.95. Noting that $\|\tilde{\boldsymbol{n}}\|_2^2 \sim \chi^2_{2(K-N)}$, i.e., chi-squared with $2(K-N)$ degrees of freedom, we have $\epsilon^2 = \chi^2_{2(K-N)}(0.95)\mathcal{N}_0$, where $\chi^2_{2(K-N)}(0.95)$ is the 95th percentile of $\chi^2_{2(K-N)}$.

2) Estimate the support of $\boldsymbol{i}$ as

$$\hat{\mathcal{I}} = \{j : |\hat{i}_j|^2 > \mathcal{N}_0\} \tag{12}$$

3) Let $\hat{m} = |\hat{\mathcal{I}}|$ and $l[j]$ be the position of j in the ordered set $\hat{\mathcal{I}}$, i.e., $1 \le l[j] \le m$. Create the $(K-N)\times m$ selection matrix $\boldsymbol{S}$ with elements $s_{jl[j]} = 1$ for $j \in \hat{\mathcal{I}}$ and zero otherwise, and solve the conventional least-squares (LS) problem

$$\min \|\boldsymbol{w} - \boldsymbol{F}_1\boldsymbol{S}\boldsymbol{i}\|_2 \tag{13}$$

to obtain the CS-LS estimate $\hat{\boldsymbol{i}}_{\rm ls}$. That is, letting $\boldsymbol{A} = \boldsymbol{F}_1\boldsymbol{S}$, we have

$$\hat{\boldsymbol{i}}_{\rm ls} = \boldsymbol{S}(\boldsymbol{A}^H\boldsymbol{A})^{-1}\boldsymbol{A}^H\boldsymbol{w}\ . \tag{14}$$

IV. Performance Analysis

In this section, we develop expressions for the error rate of coded OFDM affected by IN. We are interested in the error rate when decoding with and without IN suppression (3) and cancellation (4) is applied, respectively. We first briefly outline the methodology to estimate bit-error rate (BER) and frame-error rate (FER), and then focus on the details to account for IN and its cancellation and suppression, respectively.

A. BER and FER

We apply the methodology developed in [23], [24], which is based on the concept of error vectors. That is, we establish a set of error vectors of maximal input-Hamming weight $w_{\max}$, whose number we denote by L_e. Then, we construct the set of error vectors $\boldsymbol{q}_{j,l}$ which start at position j, $1 \le j \le L_c$, $1 \le l \le L_e$. From those we obtain the corresponding competing codewords $\boldsymbol{z}_{j,l}$ as the vectors of N modulated symbols resulting from mapping the erroneous codewords $\boldsymbol{v}_{j,l} = \boldsymbol{c} \oplus \boldsymbol{q}_{j,l}$, $1 \le j \le L_c$, $1 \le l \le L_e$. Denoting the pairwise-error probability (PEP) of deciding in favour of $\boldsymbol{z}_{j,l}$ if $\boldsymbol{x}$ was transmitted as $\mathrm{PEP}_{j,l}$, it is shown in [23], [24] that

the BER and FER for a given channel realization $\boldsymbol{H}_{\rm cyc}$ can be tightly approximated by

$$\text{BER} = \frac{1}{L_c}\sum_{j=1}^{L_c}\min\left[\frac{1}{2},\sum_{l=1}^{L_e}a_l\text{PEP}_{j,l}\right] \quad (15)$$

$$\text{FER} = 1-\prod_{j=1}^{L_c}\max\left[0,1-\sum_{l=1}^{L_e}\text{PEP}_{j,l}\right], \quad (16)$$

where a_l is the number of bit errors for error vector l.

B. Pairwise Error Probability

1) IN Cancellation: We consider the vector $\boldsymbol{y}$ from (4). Applying the DFT operation as in conventional OFDM, we obtain

$$\boldsymbol{u} = \boldsymbol{F}_2\boldsymbol{y} = \boldsymbol{H}\boldsymbol{x} + \tilde{\boldsymbol{n}} + \boldsymbol{d}\,, \quad (17)$$

where $\boldsymbol{H} = \boldsymbol{F}_2\boldsymbol{H}_{\rm cyc}\boldsymbol{F}_2^H$ is an $N\times N$ diagonal matrix of complex channel gains for the N active subcarriers, $\tilde{\boldsymbol{n}} = \boldsymbol{F}_2\boldsymbol{n}$ is AWGN, and $\boldsymbol{d} = \boldsymbol{F}_2(\boldsymbol{i}-\hat{\boldsymbol{i}}_{\rm ls})$ is the residual distortion by IN in the frequency domain. As in conventional coded OFDM, decoding is performed based on the vector metric $\|\boldsymbol{u}-\boldsymbol{H}\boldsymbol{x}\|_2$ using the Viterbi algorithm.

For the following, we consider the two special cases of $\boldsymbol{d} = \boldsymbol{F}_2\boldsymbol{i}$, i.e., no IN cancellation, and $\boldsymbol{d} = \boldsymbol{0}$, i.e., perfect IN cancellation. We further assume that i_j for $j\in\mathcal{I}$ is Gaussian distributed with variance σ_i^2. Then, standard analysis shows that the PEP is given by

$$\text{PEP}_{j,l} = \text{Q}\left(\frac{\|\boldsymbol{H}(\boldsymbol{x}-\boldsymbol{z}_{j,l})\|_2^2}{\|\boldsymbol{L}\boldsymbol{H}(\boldsymbol{x}-\boldsymbol{z}_{i,l})\|_2}\right), \quad (18)$$

where $\text{Q}(\cdot)$ is the Gaussian-Q function and $\boldsymbol{L} = \sqrt{2}\left(\mathcal{N}_0\boldsymbol{I}_K+\xi(\boldsymbol{I}_K-\boldsymbol{E})\right)^{1/2}\boldsymbol{F}_2^H$ with $\xi=\sigma_i^2$ (no cancellation) and $\xi=0$ (perfect cancellation), respectively, and the $K\times K$ identity matrix $\boldsymbol{I}_K$.

2) Erasure Decoding: We now consider the vector $\boldsymbol{y}$ from (3) and assume that the IN $\boldsymbol{i}$ is completely suppressed. Applying the DFT operation, we obtain

$$\begin{aligned}\boldsymbol{u} = \boldsymbol{F}_2\boldsymbol{y} &= \boldsymbol{F}_2\boldsymbol{E}\boldsymbol{H}_{\rm cyc}\boldsymbol{F}_2^H\boldsymbol{x}+\tilde{\boldsymbol{n}}\\ &= \boldsymbol{F}_2\boldsymbol{E}\boldsymbol{F}_2^H\boldsymbol{H}\boldsymbol{x}+\tilde{\boldsymbol{n}}\,,\end{aligned} \quad (19)$$

where now $\tilde{\boldsymbol{n}} = \boldsymbol{F}_2\boldsymbol{E}\boldsymbol{n}$. While decoding such that $\|\boldsymbol{u}-\boldsymbol{F}_2\boldsymbol{E}\boldsymbol{F}_2^H\boldsymbol{H}\boldsymbol{x}\|_2$ is maximized was optimal, we refrain from considering this option as it would require joint decoding of codewords $\boldsymbol{c}$, whose complexity is exponential in L_c. Instead, we assume conventional Viterbi decoding based on $\|\boldsymbol{u}-\boldsymbol{H}\boldsymbol{x}\|_2$ with complexity is linear in L_c. The corresponding PEP can be derived as

$$\text{PEP}_{j,l} = \text{Q}\left(\frac{\frac{1}{2}\|\boldsymbol{H}(\boldsymbol{x}-\boldsymbol{z}_{j,l})\|_2^2+\Re\{\boldsymbol{x}^H\boldsymbol{M}(\boldsymbol{x}-\boldsymbol{z}_{j,l})\}}{\sqrt{(1/2\mathcal{N}_0\|(\boldsymbol{F}_2\boldsymbol{E})^H\boldsymbol{H}(\boldsymbol{x}-\boldsymbol{z}_{i,l})\|_2}}\right), \quad (20)$$

where $\boldsymbol{M} = \boldsymbol{H}^H(\boldsymbol{F}_2\boldsymbol{E}\boldsymbol{F}_2^H-\boldsymbol{I}_K)\boldsymbol{H}$.

V. Results and Discussion

In this section, we present and discuss numerical results to illustrate the effect of IN on coded OFDM transmission and the effectiveness of CS-based IN detection for IN mitigation.

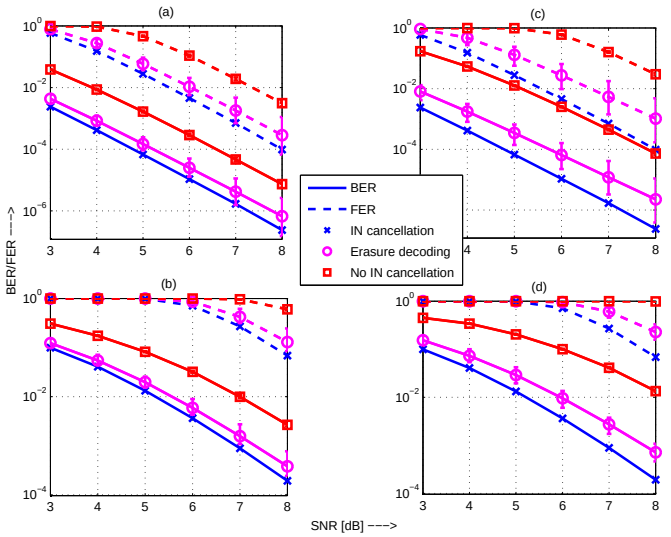

Fig. 3. BER and FER results versus SNR for coded OFDM over PLC channels. The vertical bars for "erasure decoding" and "no IN cancellation" indicate the spread of results as function of the location of the IN block. (a) Channel realization 1, $m=30$ IN samples, (b) Channel realization 2, $m=30$ IN samples, (c) Channel realization 1, $m=60$ IN samples, (d) Channel realization 2, $m=60$ IN samples. INR = 13 dB.

A. System Parameters

We adopt the transmission mask of the IEEE 1901 OFDM physical layer shown in Figure 2. Assuming a 30 MHz noise-rejection filter at the receiver, we have $K=1224$ OFDM subcarriers in the transmission band, of which 917 would be active according to the tone mask. We null another 31 subcarriers, located uniformly across active subbands, so that $N=886$ subcarriers are active (i.e., 3% less than in IEEE 1901). The reason for this is to improve the LS estimation step (13). For the error rate results we assume 4QAM transmission and the commonly used rate-1/2 memory-6 convolutional code with generator polynomials $(133_8, 171_8)$ in octal basis.

We use the channel model presented in [16], which is representative of indoor PLC channels. The signal-to-noise power ratio (SNR) is defined as $\bar{E}_{\rm b}/\mathcal{N}_0$, where $\bar{E}_{\rm b}$ is the average received energy per information bit, where averaging is done over 1000 generated channel realizations. The IN is assumed as a single block of m samples, which are i.i.d. zero-mean Gaussian distributed with variance σ_i^2. The IN-to-noise power ratio (INR) is defined as $\text{INR}=\sigma_i^2/\mathcal{N}_0$.

B. IN Mitigation and Error-rate Performance

Figure 3 shows a set of FER (dashed lines) and BER (solid lines) results obtained with the analysis presented in Section IV. In particular, we consider no and perfect IN cancellation (Section IV-B1) and erasure decoding with perfect knowledge of $\mathcal{I}$ (Section IV-B2). The different subplots correspond to two different channel realizations (subplots (a) and (c) are for channel realization 1, subplots (b) and (d) are for channel realization 2) and an IN block size of $m=30$ (subplots (a) and (b)) and $m=60$ (subplots (c) and (d)) samples, respectively. The location of the INR block is varied within the OFDM symbol, and the corresponding spread of

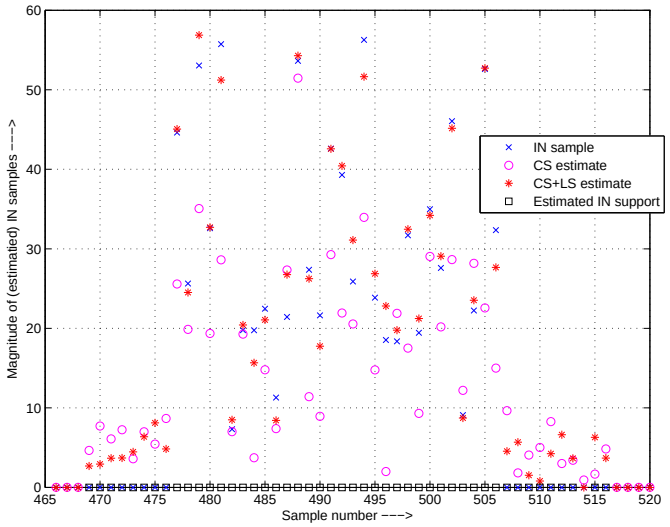

Fig. 4. Illustration of CS-based IN estimation for a single IN realization. $m = 30$ IN samples, $\mathrm{INR} = 30$ dB, and detection block-size $\delta = 12$.

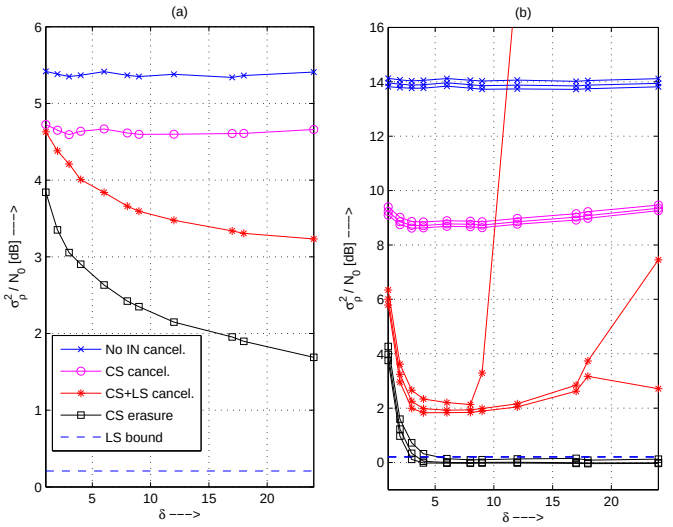

Fig. 5. Normalized empirical residual interference-plus-noise variance $\sigma_\rho^2/\mathcal{N}_0$ versus detection block-size δ for CS-based IN suppression. "LS bound" is $\sigma^2_{\rho,\mathrm{genie}}/\mathcal{N}_0$ from (22). $m = 30$ IN samples. (a) $\mathrm{INR} = 20$ dB. (b) $\mathrm{INR} = 30$ dB. The three curves for each set of results correspond to the 80%, 90%, and 100% best results $\boldsymbol{\rho}$ considered for the empirical variance σ_ρ^2.

FER and BER results is shown by vertical bars in Figure 3. The INR is chosen as $\mathrm{INR} = 13$ dB.

Comparing the results for the two channel realizations (subplots (a) and (c) versus subplots (b) and (d)) we note the FER/BER performance variations due to different channel realizations, as well as some difference in the effect of impulse noise. This demonstrates the importance of a per-realization error-rate analysis to capture the effects of channel transfer function and IN on performance of coded OFDM.

Considering the different IN mitigation options, we observe that ideal erasure decoding, i.e., when $\hat{\mathcal{I}} = \mathcal{I}$, leads only to small performance degradations compared to perfectly removed IN. The degradation is due to the removal of signal energy when erasing IN-corrupted received samples. However, compared to the case of unprocessed IN, the performance loss is fairly moderate. Note that the 'no IN cancellation' curves in Figure 3 would degrade further with increasing INR, while erasure decoding is insensitive to the INR. Furthermore, even with $m = 60$ erased symbols, the performance of erasure decoding is only moderately degraded.

Clearly, detection without IN cancellation suffers from a notable performance degradation, which is roughly proportional to the increase in overall noise-plus-interference power by a factor $(1+\mathrm{INR})$ compared to the perfect IN-cancellation case.

In summary, the exemplary results shown in this section suggest that besides perfect IN cancellation, which of course is most desirable, erasure decoding is a promising approach to mitigate the effect of IN. Key for erasure decoding to be effective is the successful identification of IN-corrupted received samples.

C. CS-based Detection

We now turn to the task of IN identification and cancellation using the CS-based detection procedure described in Section III-C.

Figure 4 shows the magnitude of IN samples i_j, the "raw" CS estimate $\hat{i}_j$ from (11), and the LS processed estimate $\hat{i}_{\mathrm{ls},j}$ from (14) for the relevant range of time-domain sample index j for an IN example with $m = 30$, $\mathrm{INR} = 30$ dB, and block-based CS with $\delta = 12$. Also shown are the estimated IN support $\hat{\mathcal{I}}$ from (12). We observe that the IN block is well identified through CS detection. In particular, all IN-corrupted samples are identified as such. Some "clean" samples are also labeled as corrupted, i.e., $\mathcal{I} \subset \hat{\mathcal{I}}$, but as seen in the previous section, this would not be dramatic in case of erasure decoding. Furthermore, the LS estimate $\hat{\boldsymbol{i}}_{\mathrm{ls}}$ is fairly close to the true IN $\boldsymbol{i}$, allowing also effective IN cancellation. In the shown example, the residual IN energy $\|\hat{\boldsymbol{i}}_{\mathrm{ls}} - \boldsymbol{i}\|_2^2$ is only 3% of the IN energy $\|\boldsymbol{i}\|_2^2$.

Next, we consider the reduction of IN energy due to block-based CS. To this end, we define the residual interference-plus-noise signal

$$\boldsymbol{\rho} = \boldsymbol{i} + \boldsymbol{n} - \begin{cases} \hat{\boldsymbol{i}}, & \text{for CS} \\ \hat{\boldsymbol{i}}_{\mathrm{ls}}, & \text{for CS+LS} \end{cases} . \tag{21}$$

In case of known support, i.e., genie-aided IN detection with $\hat{\mathcal{I}} = \mathcal{I}$, the variance of $\boldsymbol{\rho}$ for LS estimation is given by [8]

$$\sigma^2_{\rho,\mathrm{genie}} = \frac{\mathcal{N}_0}{K} \mathrm{trace}\{\boldsymbol{I} + \boldsymbol{S}\boldsymbol{B}^{-1}\boldsymbol{S}^H - \boldsymbol{S}\boldsymbol{B}^{-1}\boldsymbol{C}^H - \boldsymbol{C}\boldsymbol{B}^{-1}\boldsymbol{S}^H\} , \tag{22}$$

where $\boldsymbol{B} = \boldsymbol{S}^H\boldsymbol{F}_1^H\boldsymbol{F}_1\boldsymbol{S}$ and $\boldsymbol{C} = \boldsymbol{F}_1^H\boldsymbol{F}_1\boldsymbol{S}$.

Figure 5 shows the normalized empirical residual noise variance $\sigma_\rho^2/\mathcal{N}_0$ based on 500 IN realizations as function of the block-size δ of block-based CS for the case of $m = 30$ and (a) $\mathrm{INR} = 20$ dB and (b) $\mathrm{INR} = 30$ dB. In case of "CS erasure", $\rho_j = 0$ for $j \in \hat{\mathcal{I}}$. Also included is $\sigma^2_{\rho,\mathrm{genie}}$ from (22), labeled as "LS bound". Let us first consider Figure 5(a) for $\mathrm{INR} = 20$ dB. It can be seen that block-based CS is able to notably reduce the variance of residual interference and noise. In particular, the estimation of the IN support is fairly successful, which leads to a significant reduction of

interference when IN suppression ("CS erasure") or the LS-step (13) ("CS+LS cancel.") are applied. Increasing the block-size $\delta > 1$, i.e., using block-based instead of conventional CS, clearly helps for the considered scenario of bursty IN. When erasing signal samples, of course also part of the desired signal is removed. But we note that for the results shown in Figure 5(a), the *maximum* number of erasures observed was $|\hat{\mathcal{I}}| = [20, 30, 38, 41, 47, 47]$ for $\delta = [1, 4, 8, 12, 18, 24]$ and thus the loss in signal energy is well compensated by the gain from suppressing IN.

The results of CS-based are even more impressive if the INR increases; that is, when strong IN occurs. While this deteriorates error-rate performance for conventional detectors, this is not so for CS-based IN detection, since a larger INR facilitates detection of IN-corrupted samples. In Figure 5(b), for each set of CS results, the empirical variance σ_ρ^2 is plotted considering the 80%, 90%, and 100% (i.e., all) realizations of $\boldsymbol{\rho}$ with the smallest magnitude $\|\boldsymbol{\rho}\|_2$. We observe a huge reduction in residual interference and noise due to the proposed CS scheme. Again, block-based CS improves notably over conventional CS. The three different curves for each type of CS results are all bunched up except for the case of LS estimation. In this case, the empirical variance increases sharply for block-sizes δ beyond some threshold. But we note from the divergence of the three curves for LS that this increase in residual error is not experienced for all IN realizations, but only for a minority of cases. This at first glance strange behaviour can be explained by the fact that the matrix $\boldsymbol{A}^H\boldsymbol{A}$ in (14) can be ill-conditioned depending on $\hat{\mathcal{I}}$. A remedy for this problem would be the selection of different null-subcarriers for IN detection, which in our example have been dictated by the transmission mask. Finally, we again note that erasure decoding could be the method of choice, since the $\mathcal{I} \subseteq \hat{\mathcal{I}}$ for most cases. The maximum number of erasures observed in the 500 test runs was $|\hat{\mathcal{I}}| = [62, 61, 77, 81, 83]$ for $\delta = [4, 8, 12, 18, 24]$. While these are larger than for $\mathrm{INR} = 20$ dB, the significant gains due to IN suppression will clearly offset the loss in desired signal energy in most cases.

VI. Conclusions

Impulse noise (IN) is a serious problem for reliable PLC transmission. For sufficiently broadband PLC systems, IN occurs in bursts. In this paper, we have proposed the application of block-based CS to detect such bursts, making use of OFDM null-subcarriers. This includes the recovery of the support of the non-zero IN samples, for IN suppression, and the actual reconstruction of IN samples, for IN cancellation. Numerical results have shown that block-based CS can successfully find IN bursts and provide good estimates of IN realizations. Furthermore, by means of an error-rate analysis for coded OFDM we have demonstrated that erasure decoding, making use of CS-based IN suppression, is a promising approach to mitigate the impact of IN. The block size δ for block-based CS should be chosen such that the error correction code can cope with a number of erasures about two to three times the block size.

References

[1] M. Zimmermann and K. Dostert, "An analysis of the broadband noise scenario in powerline networks," in *Intl. Symp. Power Line Commun. (ISPLC)*, Limerick, Ireland, Apr. 2000, pp. 131–138.

[2] ——, "Analysis and modeling of impulsive noise in broadband powerline communications," *IEEE Trans. Electromagn. Compat.*, vol. 44, no. 1, pp. 249–258, Feb. 2002.

[3] H. Ferreira, L. Lampe, J. Newbury, and T. S. (Editors), *Power Line Communications*. John Wiley & Sons, 2010.

[4] S. Zhidkov, "Analysis and comparison of several simple impulsive noise mitigation schemes for OFDM receivers," *IEEE Trans. Commun.*, vol. 56, no. 1, pp. 5–9, Jan. 2008.

[5] J. Mitra and L. Lampe, "Convolutionally coded transmission over Markov-Gaussian channels: Analysis and decoding metrics," *IEEE Trans. Commun.*, vol. 58, no. 7, pp. 1939–1949, July 2010.

[6] J. Häring and A. Vinck, "OFDM transmission corrupted by impulsive noise," in *Intl. Symp. Power Line Commun. (ISPLC)*, Limerick, Ireland, Apr. 2000, pp. 9–14.

[7] H. Matsuo, D. Umehara, M. Kawai, and Y. Morihim, "An iterative detection scheme for OFDM over impulsive noise channels," in *Intl. Symp. Power Line Commun. (ISPLC)*, Athens, Greece, Mar. 2002.

[8] G. Caire, T. Al-Naffouri, and A. Narayanan, "Impulse noise cancellation in OFDM: An application of compressed sensing," in *IEEE Intl. Symp. Information Theory (ISIT)*, Toronto, Canada, July 2008, pp. 1293 – 1297.

[9] E. Candés, J. Romberg, and T. Tao, "Robust uncertainty principles: Exact signal resonstruction from highly incomplete frequency information," *IEEE Trans. Inform. Theory*, vol. 52, no. 2, pp. 489–509, Feb. 2006.

[10] D. Donoho, "Compressed sensing," *IEEE Trans. Inform. Theory*, vol. 52, no. 4, pp. 1289–1306, Mar. 2006.

[11] E. Candés and M. Wakin, "An introduction to compressive sampling," *IEEE Signal Processing Mag.*, vol. 25, no. 2, pp. 21–30, Mar. 2008.

[12] M. Luby, M. Watson, T. Gasiba, and T. Stockhammer, "High-quality video distribution using power line communication and aplication layer forward error correction," in *Intl. Symp. Power Line Commun. (ISPLC)*, Pisa, Italy, Apr. 2007, pp. 431–436.

[13] M. Stojnic, F. Parvaresh, and B. Hassibi, "On the reconstruction of block-sparse signals with an optimal number of measurements," *IEEE Trans. Signal Processing*, vol. 57, no. 8, pp. 3075–3085, Aug. 2009.

[14] Y. Eldar, P. Kuppinger, and H. Bölcskei, "Block-sparse signals: Uncertainty relations and efficient recovery," *IEEE Trans. Signal Processing*, vol. 58, no. 6, pp. 3042–3054, June 2010.

[15] Broadband over power lines PHY/MAC working group of the IEEE Communications Society, "IEEE P1901™/D3.00 - Draft standard for broadband over power line networks: Medium access control and physical layer specifications," Feb. 2010.

[16] A. Tonello, "Wideband impulse modulation and receiver algorithms for multiuser power line communications," *EURASIP Journal on Advances in Signal Processing*, vol. 2007, no. Article ID 96747, 2007.

[17] R. Fischer, *Mehrkanal- und Mehrträgerverfahren für die schnelle digitale Übertragung im Ortsanschlußleitungsnetz*. Aachen, Germany: Shaker Verlag, 1997.

[18] S. Wei, D. Goeckel, and P. Kelly, "Convergence of the complex envelope of bandlimited OFDM signals," *IEEE Trans. Inform. Theory*, vol. 56, no. 10, pp. 4893–4904, Oct. 2006.

[19] D. L. Donoho, M. Elad, and V. N. Temlyakov, "Stable recovery of sparse overcomplete representations in the presence of noise," *IEEE Trans. Inform. Theory*, vol. 52, no. 1, pp. 6–18, 2006.

[20] E. Candés, J. Romberg, and T. Tao, "Stable signal recovery from incomplete and inaccurate measurements," *Communications on Pure and Applied Mathematics*, vol. 59, no. 8, pp. 1207–1223, Aug. 2006.

[21] E. Candés and P. Randall, "Highly robust error correction by convex programming," *IEEE Trans. Inform. Theory*, vol. 53, no. 7, pp. 2829–2840, July 2008.

[22] A. Oka and L. Lampe, "A compressed sensing receiver for UWB impulse radio in bursty applications like wireless sensor networks," *Elsevier Physical Communication, Special Issue on Advances in Ultra-Wideband Wireless Communications*, vol. 2, no. 4, pp. 268–264, Dec. 2009.

[23] C. Snow, L. Lampe, and R. Schober, "Error rate analysis for coded multicarrier systems over quasi-static fading channels," *IEEE Trans. Commun.*, vol. 55, no. 9, pp. 1736–1746, Sept. 2007.

[24] M. Mohammadnia-Avval, C. Snow, and L. Lampe, "Error rate analysis for bit-loaded coded MIMO-OFDM," *IEEE Trans. Veh. Technol.*, vol. 59, no. 5, pp. 2340–2351, June 2010.